

Article

Application of Graphene Oxide–Natural Polymer Composite Adsorption Materials in Water Treatment

Jiliang Xie

Institute of Marine Research Development, Jiangsu Ocean University, Lianyungang 222005, China; jiliangxie@jou.edu.cn

Abstract: Graphene is a new type of carbon material with excellent properties that has been developed in recent years. Graphene composites have potential application value in solving the problem of water pollution. In this study, we investigated the properties and performance of graphene composites prepared through polymer modification and inorganic particle doping modification. Our research focused on the composites' ability to adsorb heavy metal ions and degrade organic compounds through photocatalysis. In this study, we prepared graphene oxide (GO) first and then grafted p-phenylenediamine onto its surface. The process was successful and yielded promising results. The aniline grafted onto the graphene oxide surface was used as anchor point for the in situ redox polymerization of aniline, and a polyaniline macromolecular chain was grafted onto the edge of graphene oxide. The structure of the composite was determined using Fourier transform infrared spectroscopy, thermogravimetry, X-ray diffraction, and Raman spectroscopy and transmission electron microscopy. The adsorption performance of Pb^{2+} on GO-PANI composite was studied. The maximum adsorption capacity of the GO-PANI composite for Pb^{2+} is 1416 mg/g, 2.3 times that of PANI. Graphene/polyaniline composites can be used as an excellent adsorbent for Pb^{2+} heavy metal ions and have great application prospects in heavy metal wastewater treatment.

Keywords: graphene; polyaniline; adsorption; water treatment



Citation: Xie, J. Application of Graphene Oxide–Natural Polymer Composite Adsorption Materials in Water Treatment. *Symmetry* **2023**, *15*, 1678. <https://doi.org/10.3390/sym15091678>

Academic Editors: Bradha Madhavanh, Sung-Chul Yi and Takashiro Akitsu

Received: 23 March 2023

Revised: 16 August 2023

Accepted: 24 August 2023

Published: 31 August 2023



Copyright: © 2023 by the author. Licensee MDPI, Basel, Switzerland. This article is an open access article distributed under the terms and conditions of the Creative Commons Attribution (CC BY) license (<https://creativecommons.org/licenses/by/4.0/>).

1. Introduction

Graphene is a honeycomb two-dimensional planar carbon nanomaterial composed of only one thick carbon atom, so it has a theoretical specific surface area of more than 2600 m²/g and can realize the absorption and desorption of various substances [1]. It can be challenging to synthesize a single layer of graphene, but even graphene with a small number of layers can have a significant specific surface area after ultrasonic treatment. This results in higher adsorption capacity than that of typical adsorption materials. The precursor graphene monoxide surface has many functional groups such as epoxy groups. These functional groups are hydrophilic and can form hydrogen bonds or donor–acceptor complexes with many substances, thus introducing other functional groups or new substances to further enhance water solubility, adsorption capacity and endow graphene with new characteristics [2]. Although the unique two-dimensional structure of graphene endows it with its own unique properties, it has serious agglomeration. It can be challenging for graphene to fulfill its potential when it consists of dozens or even hundreds of layers [3]. Currently, scientists and researchers are focusing on creating graphene with only a few layers or even a single layer, ensuring high purity and minimal structural defects. Their synthesis methods are also different. At present, more mature preparation methods are mainly micromechanical stripping, solvent stripping, chemical vapor deposition (CVD), epitaxial growth, and chemical redox [4]. GO was used to investigate using group absorption, a kinetic absorption model, a model based on isotherms, and the van't Hoff equation.

To prepare GO, perchlorate is commonly used as an oxidant. It is added to a mixture containing fuming nitric acid and graphite. This process creates graphene oxide. The

reaction system is first maintained at 0 °C and then heated to 60–80 °C, and the reaction system is continuously stirred for about 24 h [5]. The oxidation degree of the product obtained using this method is relatively low. If aiming to obtain graphite oxide with a higher oxidation degree, it may be necessary to extend the reaction time. However, it is essential to note that using perchlorate as an oxidant in the reaction process can pose a certain level of risk [6]. The method of preparation of GOES using the Brodie method has an advantage in that the oxidation degree can be controlled with the oxidation time. Through the optimization and improvement of this method, the preparation of graphene oxide can be achieved more efficiently. Using perchlorate as an oxidant, graphite powder is acidified with a mixed concentrated sulfuric acid and fuming nitric acid. During the reaction, the temperature of the system is maintained at 0 °C, and the reaction time is about 56 h. The reaction time of this method is relatively long, and the oxidation degree of the product obtained is also very low [7]. If an attempt is made to improve the oxidation degree by prolonging the reaction time, the carbon layer of the obtained product is seriously damaged. In addition, many toxic gases such as ClO₂ and NO₂ are produced in the reaction process, which also pollutes the environment. Using potassium permanganate instead of perchlorate as an oxidant, graphite was oxidized using a concentrated sulfuric acid and sodium nitrate system. Using permanganate as an oxidant, the safety of the reaction was improved, and products with high oxidation degree and regular structure could be obtained. The toxic gas generated during the reaction process was relatively reduced, causing less environmental pollution [8]. Hummer's method is a popular technique for preparing GO. It is known to require an oxidation time of approximately 5 h and has significantly shortened reaction times. Hummer's method is currently one of the most widely used methods for this purpose. As a new type of carbon material with excellent performance, graphene oxide not only has a high specific surface area, but also has rich oxygen-containing functional groups on its surface, of which –OH, C=O, and COOH functional groups account for more than 60%. The high specific surface area of graphene oxide also makes it an ideal adsorption material, which can be used for treatment of environmental wastewater [9]. Moreover, compared with other carbon nanomaterials, graphene oxide has good water solubility and rich functional groups, which make its surface easy to chemically modify, and plays an important role in improving the comprehensive properties of materials. In recent years, with an increasingly serious environmental pollution problem, more and more researchers have begun to study and discuss the application of graphene oxide and its composites in environmental wastewater treatment due to its unique structure and good water solubility. The competition between adsorption–desorption of fluorescent agent rhodamine 6G and dopamine on graphene oxide was studied [10]. It was shown that graphene oxide exhibits fast adsorption performance for both organics due to its hydrophilicity and multiple oxygen-containing functional groups. There are many noncovalent forces between dopamine molecules and graphene oxide layers, including bonding and meta-m forces. However, there is only the m-m force between the rhodamine 6G and graphene oxide layer, and there is no hydrogen bond force. Therefore, in terms of dopamine and rhodamine 6G, graphene oxide has stronger adsorption capacity for the former than the latter.

In this paper, using the large specific surface area of graphene and its high adsorption capacity for aromatic ring-containing pollutants, we prepared graphene/polymer composites by edge-grafting a modified polyaniline macromolecular chain [11]. Because a polyaniline molecular chain contains many N atoms, it has a good complexing effect on heavy metals. Graphene/polyaniline composites are expected to have good adsorption performance for the heavy metal Pb (II) and have high adsorption performance for the aromatic ring contaminant methylene blue. It is a good adsorbent in wastewater treatment where heavy metals and aromatic pollutants coexist.

2. Experiments and Methods

The raw materials and processing methods used in the experiment are shown in Table 1. The experimental equipment and testing methods are shown in Tables 2 and 3, respectively.

Table 1. Raw materials and treatment methods used in the experiments.

Name	Purity	Manufacture	Remarks
Graphite	99%	Alfa	Direct use
Concentrated sulfuric acid	AR	Tianjin Chemical Reagent Company	Direct use
Fuming nitric acid	AR	Tianjin Chemical Reagent Company	Direct use
Concentrated hydrochloric acid	AR	Tianjin Chemical Reagent Company	Direct use
$KClO_3$ (potassium chlorate)	AR	Tianjin Guang fu Technology Co., Ltd.	Direct use
1-(3-dimethylaminopropyl)-3-ethylcarbodiilene	99%	Alfa	Direct use
(EDC · HCl) p-phenylenediamine	AR	Sinopharm Chemical Reagent Co., Ltd.	Direct use
N-methyl pyrrolidone (NMP)	AR	Tianjin Guang fu Fine Chemical Research Institute	Vacuum distillation
N, N-dimethylformamide (DMF)	AR	Tianjin Chemical Reagent Company	Vacuum distillation
N-hydroxy succinimide (NHS)	99%	Alfa	Direct use
Tetrahydrofuran (THF)	AR	Tianjin Chemical Reagent Company	Vacuum distillation
Aniline	AR	Beijing Bellwether Technology Co., Ltd.	Direct use
Ammonium persulfate	AR	Tianjin Guang fu Fine Chemical Research Institute	Direct use
Sodium hydroxide (NaOH)	AR	Tianjin Chemical Reagent Company	Vacuum distillation
Styrene (St)	AR	Beijing Bellwether Technology Co., Ltd.	Vacuum distillation
Methacryloyloxyethyl Trimethylammonium chloride	72%	Beijing Bellwether Technology Co., Ltd.	Direct use

Table 2. List of instruments employed for the experiments.

Instrument	Manufacturer
Nuclear magnetic resonance spectrometer	Varian, USA
Fourier infrared spectrometer	BIO-RAD
High resolution transmission electron microscope	FEI
Atomic force microscope	Nasoscope IVV atomic force microscope
Thermogravimetric analyzer	Netsch TG 209
Freeze dryer	Beijing Bokang Experimental Instrument Co., Ltd.
Ultraviolet-visible spectrophotometer	Shanghai Instrumental Analysis Instrument Co., Ltd.
X-ray diffraction analyzer	Rigaku
Fluorescence spectrophotometer	RF-5301PC
Ultraviolet visible diffuse reflectometer	Agilent
Scanning electron microscope	FEI

Table 3. List of test methods.

Characterization Instrument	Test Conditions
Thermogravimetric analyzer (TGA)	Netsch TG 209, heating rate is 10 k/min, and room temperature rises to 800 °C. Before test, sample shall be drained.
Transmission electron microscope (TEM)	JEM-100CX II transmission electron microscope, working voltage is 100 KV. First, ultrasonic dispersion of sample in organic solvent, then drop it onto copper mesh, dye sample for 8 h, and then RuO_4 for 2 h.

Table 3. Cont.

Characterization Instrument	Test Conditions
Atomic force microscope (AFM)	Nanoscope IV Atomic Force Microscope (Digital Instruments Inc.). The working mode is tapping mode. The cantilever is made of single-crystal silicon material. The resonant frequency is 320 KHz, working voltage is 2~3 V, tip radius is less than 10 nm, and scanning rate is 1.0 Hz. First, disperse ultrasound uniformly; then, drop sample on mica sheet and dry it.
FT-IR infrared spectrometer	The dried samples were pressed with KBr and tested on Bio Rad fts6000 Fourier infrared spectrometer
X-ray diffraction analyzer (XRD)	D/max-2500 diffractometer, power 3 kW, $CuK\alpha$ as radiation ($\lambda = 1.5406 \text{ \AA}$), scanning rate 2% min, scanning range $5^\circ \sim 100^\circ$
Scanning electron microscope (SEM)	The FeinanoSEM450 field emission scanning electron microscope from EDA X Company is adopted
Ultraviolet-visible diffuse reflection spectrum, UV-vis DRS	Cary5000 ultraviolet visible diffuse reflectance spectrometer of Agilent Company was used for testing. Barium sulfate was used as standard white plate (100% T), scanning speed was 600 nm/min, scanning wavelength range was 200–800 nm, and scanning step was 2 nm

2.1. Preparation of GO

The graphene oxide (GO) used in the experiment was chemically oxidized and prepared according to the Staudenmaier method [12]. First, weigh and disperse graphite (8.0 g) into mixed solution of concentrated H_2SO_4 (72 mL) and concentrated HNO_3 (140 mL), place it in an ice bath for mechanical stirring, and then slowly add $KClO_3$ (88 g). After 7 days of reaction, first dilute it with water, and then wash it with 5% HCl to remove sulfate radicals. A length of 1400 μm /710 μm graphite is gathered. This graphene is formed from flake graphite. Then, wash mixed product with high-purity water several times until it is neutral, place it in a vacuum oven at 60 $^\circ C$, and vacuum dry it for 24 h to obtain GO with oxygen-containing groups on its surface. Staudenmaier technique was deployed based on Brodie methodology, where an association of HNO_3 and H_2SO_4 is utilized as the intercalant forming graphite oxide with maximum ratio of C/O. Moreover, both of these techniques depend on a long oxidation phase that requires as long as one week duration.

2.2. Preparation of GO-NH₂

Weigh GO (1 g) and put it into 100 mL of freshly evaporated DMF, ultrasonic disperse it for 24 h, place it in an ice bath, add EDC•HCl (6.0035 g) and NHS (3.084 g), remove ice bath, react overnight at room temperature, add 10 mL of DMF dissolved in p-phenylenediamine (5.1148 g), react overnight at room temperature, filter, separate filter residue and centrifuge it with water and ethanol several times, and then place product in a 50C oven and vacuum dry it for 24 h to obtain black powdery substance (GO-NH₂). DMF is utilized in various industries as a solvent and in fiber manufacturing substances including plastics and different chemicals. The evaporation pressure of DMF, which is miscible when mixed with water, is 3.5 hPa.

2.3. Preparation of GO-PANI

Weigh G-NH₂ (0.2884 g) and ultrasonic disperse it in 42 mL per 1 mol/L hydrochloric acid solution; then, add aniline (2.8 mL) and stir and mix evenly, quickly add 28 mL hydrochloric acid solution dissolved in per sulfuric acid (6.888 g), and stir it in ice bath for 6 h. Add an excessive amount of 0.5 mol/L NaOH solution; reaction solution changes from dark green to black blue; filter, centrifuge wash filter residue with a large amount of N-methyl pyrrolidone, and then mix it with 1 mol/L hydrochloric acid overnight, dry product in a 60C vacuum oven, and obtain GO-PANI with black green powder in conductive state. Initiation is the primary phase of the polymerization procedure; during this phase, an

active point is formed from where the chain of polymers is generated. Not every monomer is susceptible to every type of initiator.

2.4. Preparation of PANI

Add 0.8 mL aniline to 12 mL of 1 mol/L hydrochloric acid solution, rapidly drop 8 mL of hydrochloric acid solution with 2 g per sulfuric acid and stir in ice bath for 6 h. Wash with excessive anhydrous ethanol, and then mix with 1 mol/L hydrochloric acid overnight. Dry product in a 60°C vacuum oven to obtain dark green conductive PANI powder.

3. Results

In this study, we used oxygen on a GO surface to attach-NH₂ of phenylenediamine as a site and then conducted oxidative graft polymerization of aniline. The authors in [13] thoroughly reviewed magnetic graphene application. The traditional PANI has a granular structure, and its morphology and performance are not as good as those of rod PANI. The main difference between the two in preparation is that the oxidant of the former is added slowly, while the oxidant of the latter is added quickly. The synthetic route of the product is shown in Figure 1. An oxidizing agent was added during the polymerization process to prepare GO-PANI nanocomposites. Figure 1 illustrates the synthesis of the nanocomposites. GO is produced as a starting point for a material with oxygen-containing functional groups. GO surfaces are then modified by attaching amino groups to compounds, such as phenylenediamine (-NH₂). The amine-functionalized GO was then oxidatively polymerized with aniline monomers. There are two cases presented, one with slow addition and one with rapid addition of the oxidizing agent. GO-PANI nanocomposite was formed by the growth of polyaniline chains on the GO surfaces. After washing to remove the unreacted components or byproducts, the nanocomposites were dried to stabilize them. Finally, various characterization techniques, such as XRD, were employed to analyze the properties of the GO-PANI nanocomposites. Figure 1 emphasizes the contrasting approaches for adding oxidizing agents at different rates and the polymerization process.

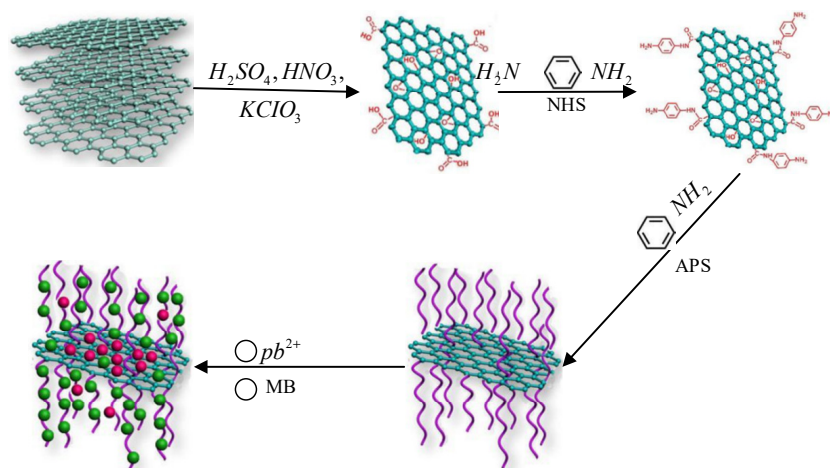


Figure 1. Schematic diagram of route for preparing GO-PANI nanocomposites.

Figure 2 is an AFM image of GO. It can be seen from the figure that the GO layer is about 0.8 nm, which is consistent with the XRD result of 0.72 nm, indicating that the graphene oxide layer is a single layer.

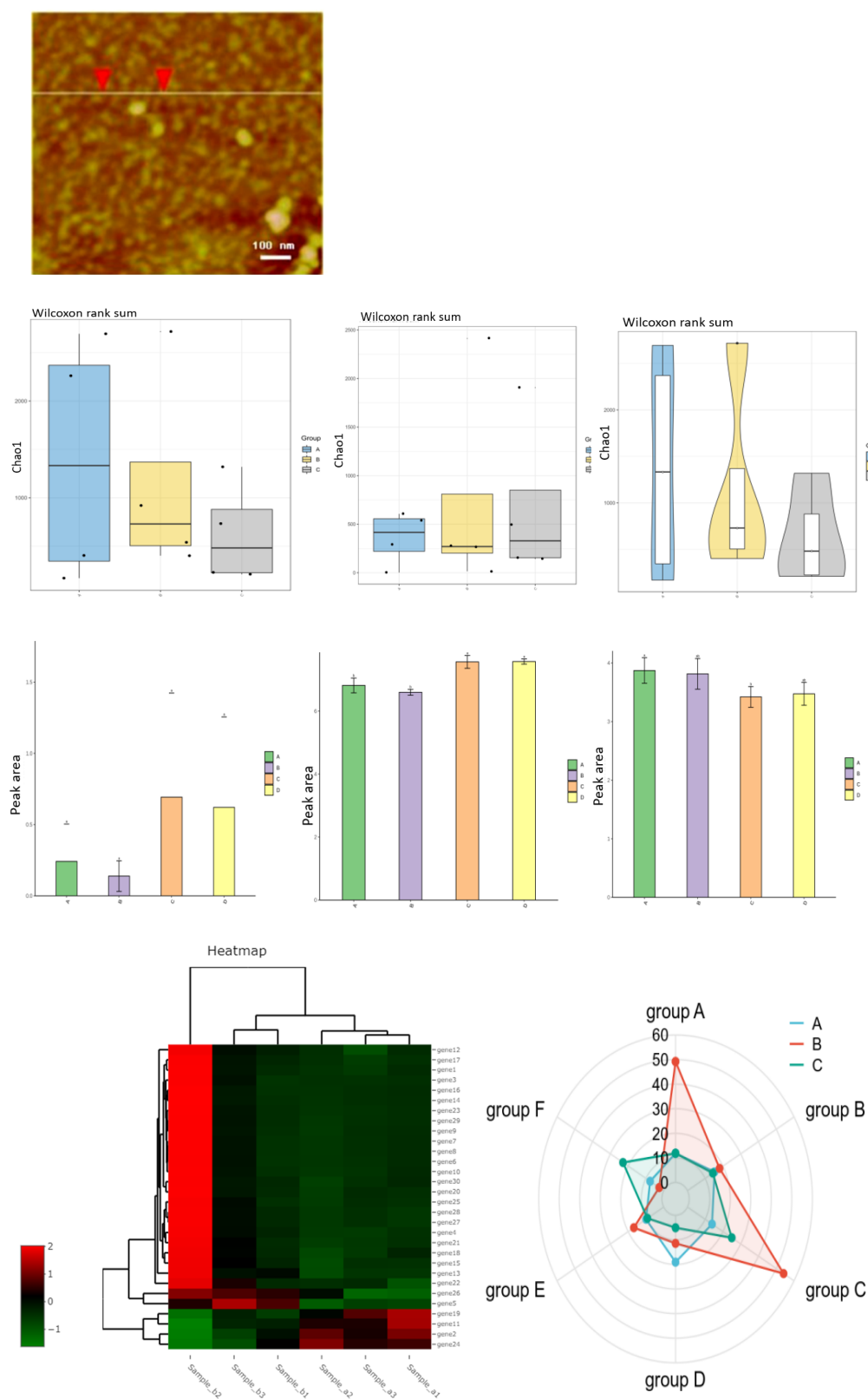


Figure 2. AFM Diagram of GO.

The composite structure was characterized using FT-IR [14]. As shown in Figure 3. Figure 3 is the infrared spectrum of GO. It can be seen from figure that a wide peak at $3000\text{--}3650\text{ cm}^{-1}$ is caused by stretching vibration of light functional groups on GO, and absorption peaks at 1725 cm^{-1} and 1645 cm^{-1} are caused by stretching vibration of carbon

GO is 0.72 nm. This peak belongs to reflection peak of 001 crystal plane, which is related to the preparation method of GO and the number of graphene layers [22]. The diffraction peak at $2\theta = 42.0^\circ$ belongs to a graphite-like structure of the graphene 100 crystal plane [23]. After reaction of p-phenylenediamine with GO, the 001 diffraction peak of graphene oxide lamella moves $2\theta = 10.2^\circ$ to low angle, and the corresponding layer spacing is 0.87 nm (Figure 4). The increase in interlayer spacing may be caused by the insertion of p-phenylenediamine and the reaction between layers [24]. At same time, in the curve of Figure 4, $2\theta = 21.3^\circ$. A new broad peak appears, which is the diffraction peak of the reduced graphene oxide. The distance between the graphene sheets is 0.42 nm. After reaction of p-phenylenediamine with GO, some GO is reduced [25]. In Figure 4, characteristic diffraction peaks of PANI appeared at $2\theta = 15.0^\circ$, $2\theta = 20.1^\circ$, and $2\theta = 25.2^\circ$, respectively, corresponding to 011020 of PANI and diffraction peaks of 200 crystal planes. In the GO-PANI composite (Figure 4), a GO characteristic diffraction peak disappears, and graphene is $2\theta = 42.0^\circ$. The characteristic peak of GO-PANI also disappears, indicating that graphene oxide in GO-PANI is in a stripped state, and there is no aggregation structure. Compared with pure PANI, a characteristic diffraction peak of PANI appears in GO-PANI, indicating that the crystallinity of PANI in composite is low.

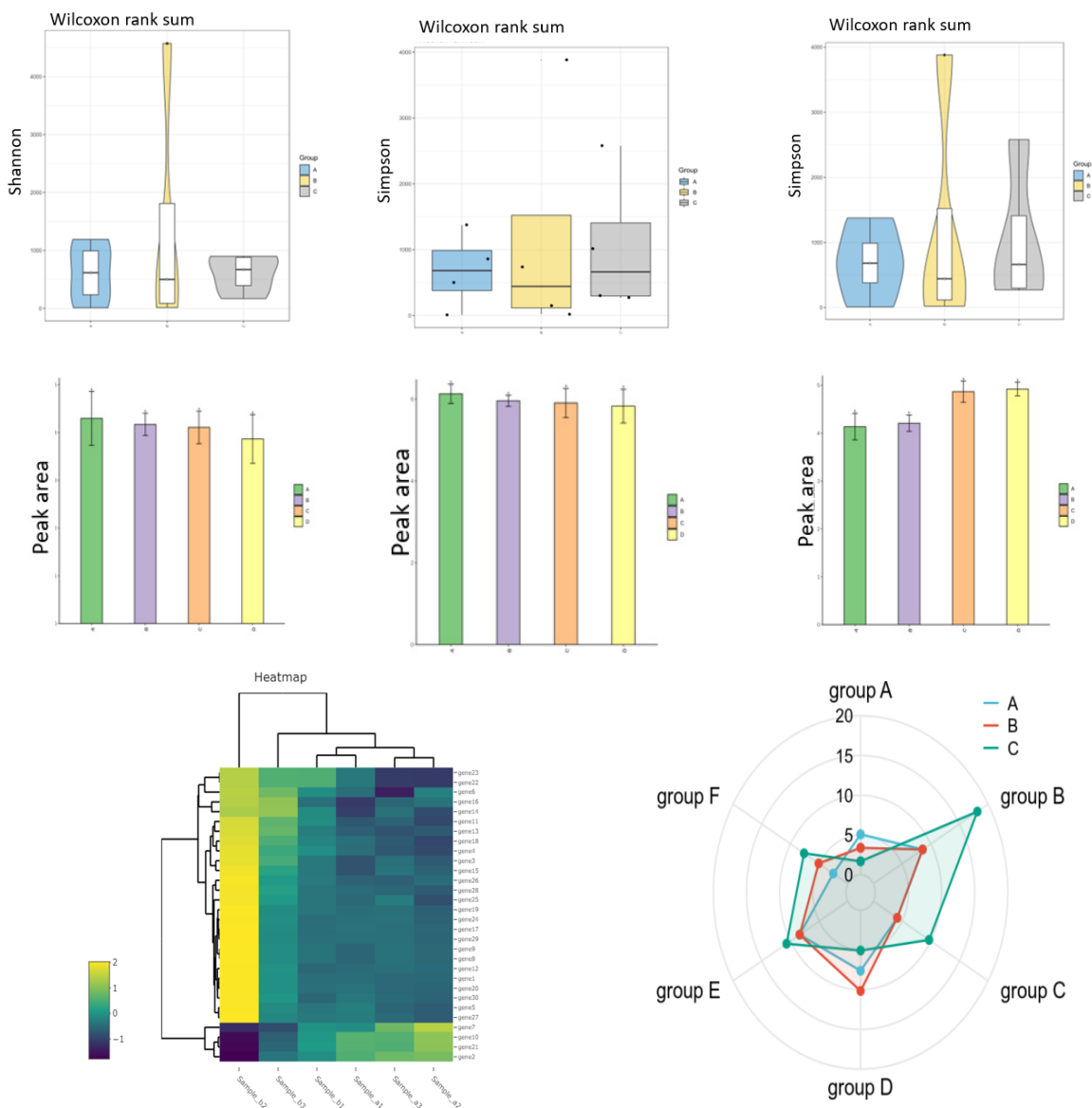


Figure 4. XRD spectrum.

Figure 5 is Raman spectrum of GO, GO-PANI, and PANI. As shown in Figure 5A, the G-band at 1598 cm^{-1} is caused by sp^2 hybrid vibration of carbon atoms in a two-dimensional graphite hexagonal system. The D-band at 1314 cm^{-1} is caused by presence of sp^3 hybrid carbon atoms due to defects in the graphene. In the GO-PANI composite (Figure 5B), compared with the GO, two new absorption peaks appeared at 1174 cm^{-1} and 1503 cm^{-1} due to the introduction of a PANI molecular chain, corresponding to awakening C–H vibration and C=C stretching vibration in the PANI, respectively. It showed that PANI was successfully grafted onto the GO layer.

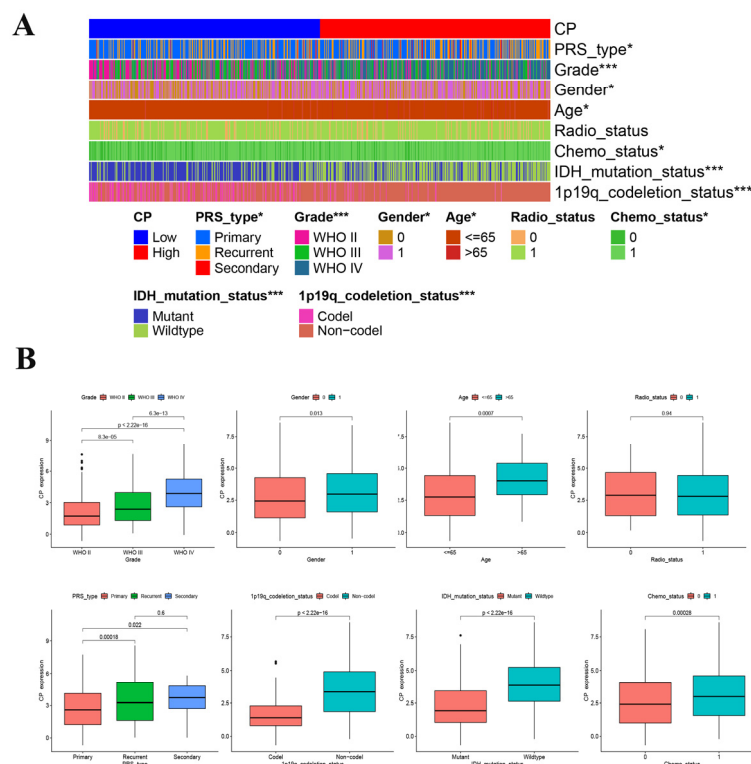


Figure 5. Raman spectrum.

Figure 6 shows TGA spectra of GO, GO-NH₂, GO-PANI, and PANI, respectively. This radar representation illustrates the temperature of thermal weight loss in different groups from Group A to Group F. Figure 6A shows the weight loss curve of the GO. It can be seen from the curve that the weight loss of GO below $150\text{ }^{\circ}\text{C}$ is about 5 wt. %, which is caused by desorption of water molecules adsorbed on the GO. The weight loss between $150\text{ }^{\circ}\text{C}$ and $600\text{ }^{\circ}\text{C}$ is about 18 wt. %, which is mainly caused by decomposition of oxygen-containing functional groups such as COOH and OH on the GO surface. When p-phenylenediamine is grafted onto the GO surface, weight loss of GO-NH₂ is about 34 wt. %, as shown in Figure 6B. Figure 6C shows the thermal weight loss curve of PANI. There are two parts of weight loss between $200\text{ }^{\circ}\text{C}$ and $600\text{ }^{\circ}\text{C}$, which are, respectively, caused by loss of doped acids on the PANI chain and the decomposition of macromolecular chains. When the PANI is grafted onto the GO surface, the initial decomposition temperature of the PANI molecular chain is about $457\text{ }^{\circ}\text{C}$, which is higher than that of the PANI ($412\text{ }^{\circ}\text{C}$). This shows that the thermal stability of the GO-PANI composite is higher than that of PANI due to the presence of GO lamella.

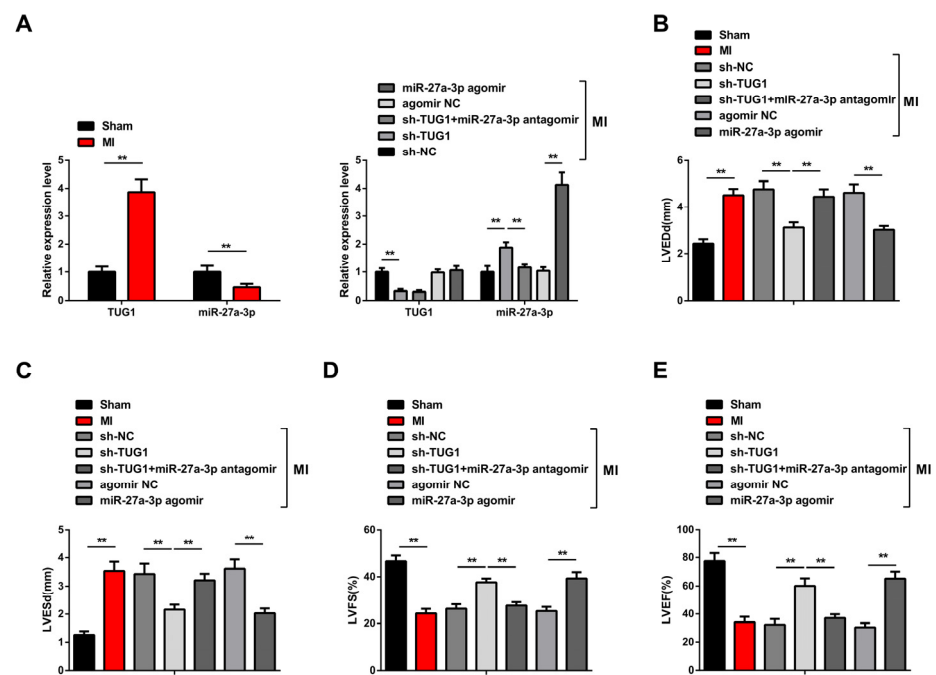


Figure 6. Thermal weight loss spectra.

TEM was used to observe the micromorphology of GO, PANI, and GO-PANI, respectively. The specific structure is shown in Figure 7. Figure 7a is a TEM diagram of synthesized GO, Figure 7b is a TEM diagram of high-magnification GO, and large slices of GO with nanometer thickness can be observed. Figure 7c is a TEM diagram of the GO-PANI composite. Due to II-II interaction, the GO-PANI composite presents a large agglomeration state, and an obvious black rod-like structure can be observed on the surface of the graphene, which is similar to the rod-like structure of pure PANI (Figure 7d).

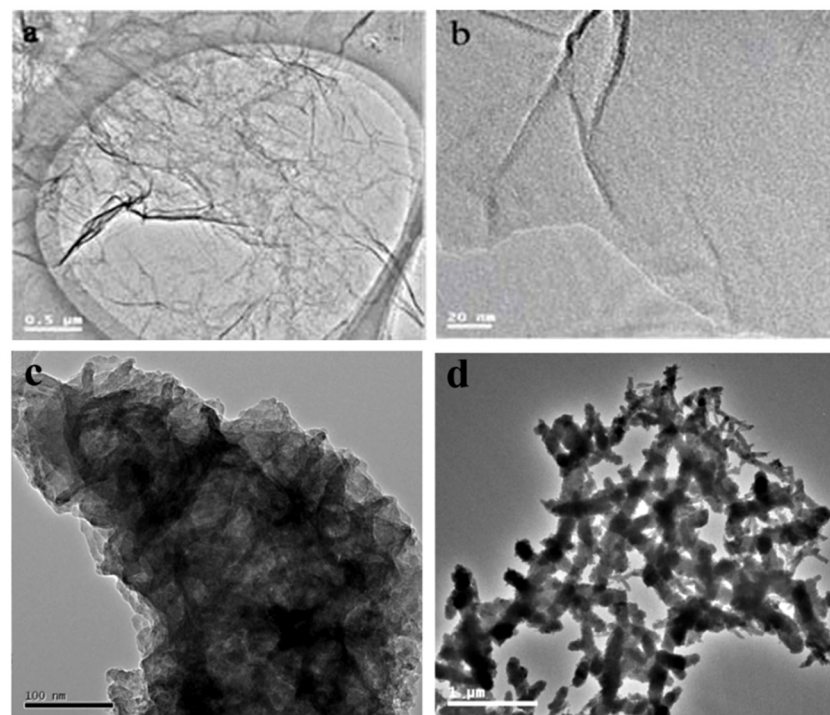


Figure 7. TEM of (a) GO; (b) modified GO; (c) GO-PAN; (d) PANI.

In this study, we examined the adsorption behavior of lead ions (Pb (II)) at different concentrations using both PANI and GO-PANI. Using these experimental data, van der Waals equation curves were plotted ($\ln(q_e/C_e)$ versus $1/T$) for both materials. As shown in Equation (1), the van der Waals equation was derived. The linear relationship between $\ln(q_e/C_e)$ and $1/T$ for PANI and GO-PANI can be seen in straight lines when plotted against $1/T$. The $-\Delta H/R$ and $\Delta S/R$ represent the slope and intercept of a straight line, respectively. Based on the results, both PANI and GO-PANI absorb lead ions effectively in water treatment applications, especially when the temperature is high. According to these findings, water purification can be achieved with graphene oxide–natural polymer composite materials.

Figures 8 and 9 are van der Waals equation curves for Pb (II) using GO-PANI and PANI, respectively. The thermodynamic parameters ΔH , ΔS , and ΔG are calculated for PANI and GO-PANI for ΔS at different temperatures. The value of $\ln(q_e/C_e)$ can be calculated from van der Waals equation.

$$\ln(q_e/C_e) = \Delta H/RT + \Delta S/R \quad (1)$$

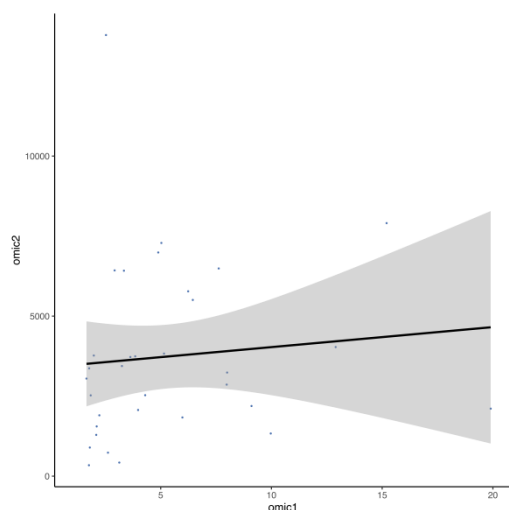


Figure 8. van der Waals equation curves of lead ions adsorption using GO-PANI.

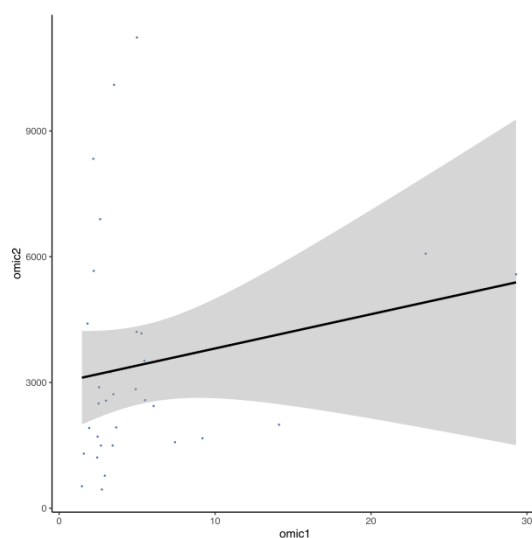


Figure 9. van der Waals equation curves of lead ions using PANI.

R refers to gas constant ($8.314 \text{ J mol}^{-1} \text{ K}^{-1}$), and T refers to absolute temperature (K). A straight line is drawn by $\ln(q_e/C_e)$ to $1/T$, and the slope and intercept of the line correspond

to $-\Delta H/R$ and $\Delta S/R$, respectively. The calculated thermodynamic parameters are listed in Table 4. ΔH is a positive value, indicating that adsorption of PANI and GO-PANI to Pb (II) is an endothermic process. The higher ΔH (ΔH 40 KJ/mol) indicates that adsorption of Pb (II) using PANI and GO-PANI is a chemisorption-dominated process. This result is consistent with quasi-second-order kinetic results. ΔS and ΔH are positive, indicating that PANI and GO-PANI absorb Pb (II), and increased temperature is conducive to the adsorption reaction.

Table 4. Thermodynamic parameters of adsorption of Pb (D) using PANI and GO-PAN at different temperatures.

	T (K)	ΔG (KJ/mol)	ΔH (KJ/mol)	ΔS (J/(mol. k))
PANI	288.0	−0.2251	49.89	170.1
	298.0	−1.966		
	308.0	−3.706		
GO-PANI	288.0	−1.151	50.34	180.1
	298.0	−3.311		
	308.0	−5.111		

The change in Gibbs free energy caused during adsorption process is calculated according to following formula:

$$\Delta G = \Delta H - T\Delta S$$

As shown in Table 4, AG is negative at 288 K, 298 K, and 308 K, indicating that adsorption of Pb (II) using PANI and GO-PANI is a spontaneous adsorption process. The AG of GO-PANI when adsorbing Pb (II) is smaller than that of PANI when adsorbing Pb (II), indicating that GO-PANI absorbs Pb (II) more easily and spontaneously than PANI.

To give full play to excellent adsorption performance of the large layer of graphene oxide on aromatic organic compounds, we grafted polyaniline on edge of graphene in this work and studied adsorption performance of GO-PANI on heavy metal ions and aromatic organic compounds in coexistence system. Figure 10 shows the co-adsorption experiment of MB (500 mg/L) and Pb (II) (250 mg/L) with 0.6 g/LPANI-GO adsorbent. The experiment shows that GO-PANI has good adsorption capacity for MB and Pb (II) in the coexistence system of MB and Pb (II), and the maximum adsorption capacity is 544 mg/g and 1004 mg/g, respectively. The adsorption capacity of GO-PANI for MB and Pb (II) alone is 734.4 mg/g and 1145 mg/g, and adsorption capacity of GO-PANI for MB and Pb (II) in the co-adsorption system is slightly lower than that in the single adsorption system, which may be the reason why the cationic dyes and metal cations compete in adsorption. When PANI is adsorbent, the maximum adsorption capacity of MB and Pb (II) in the co-adsorption system is 272 mg/g and 301 mg/g, respectively, which is slightly lower than maximum adsorption capacity of polyaniline (401 mg/g and 326 mg/g) for MB and Pb (II). The experimental results show that GOES has good adsorption capacity for MB and Pb (II) in the coexistence system after edge grafting of PANI.

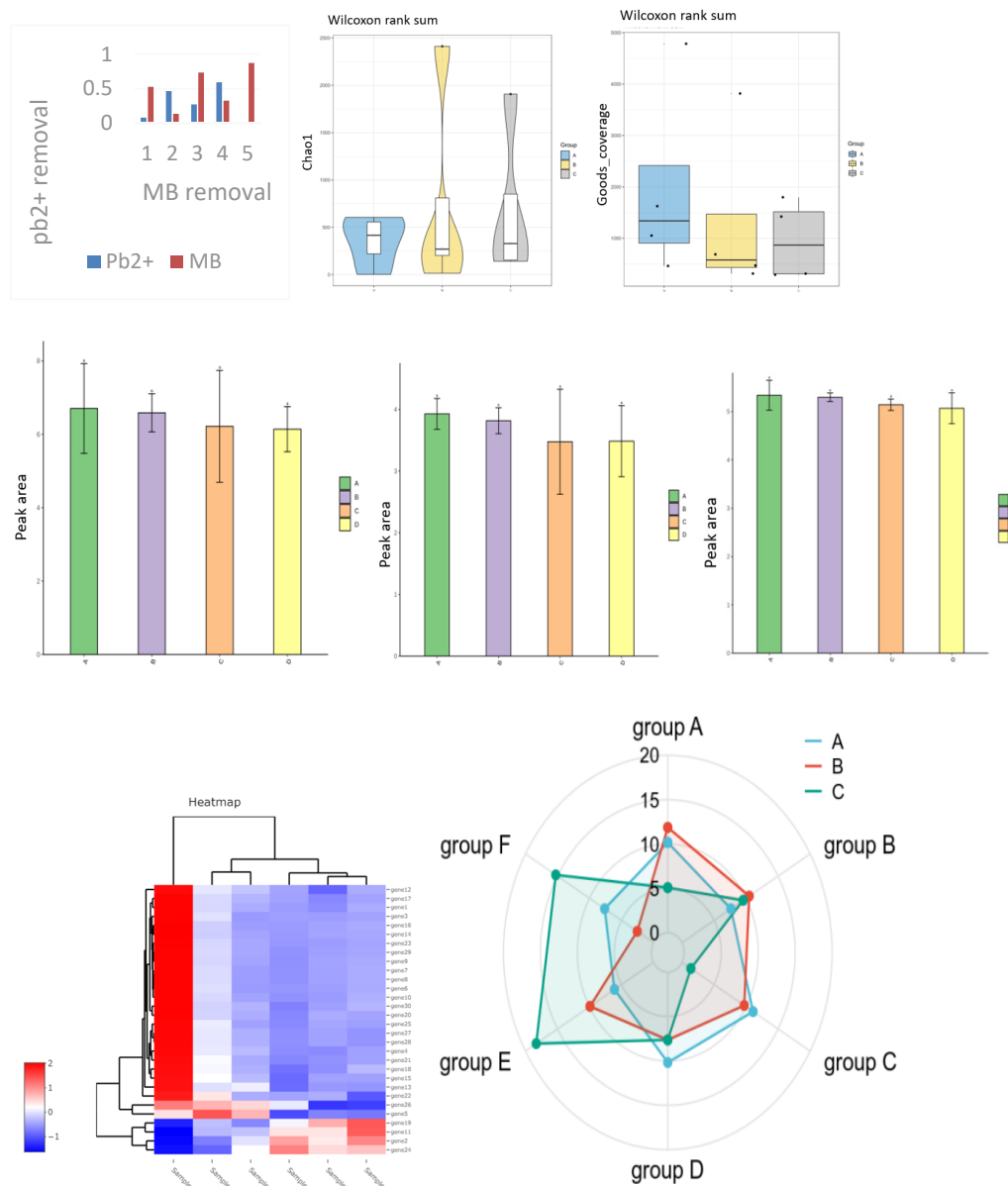


Figure 10. Effect of organic dyes on adsorption of Pb (II) using GO-PANI (adsorption dose = 0.6 g/L; pH = 6.0); initial concentration Pb (II) = 500.0 mg/L and MB = 250.0 mg/L; temperature = 298 K; adsorption time = 90 min.

4. Discussion

Water treatment with natural GO polymer composite materials has gained significant interest in recent years. There are many important characteristics associated with the two-dimensional material GO, including its large surface area, powerful adsorption capabilities, and high mechanical properties [3–10]. Integrating natural polymers further improves the environmental friendliness of this composite material for the treatment of water. As part of the treatment process, color, organic pollutants, and heavy metals are removed from the water. A substantial surface area and an affinity for adsorption make GO ideal for adsorption. Natural polymers can be added to the GO matrix to increase the adsorption capacity and selectivity of the composite adsorbent [1,6]. Natural polymers are ecofriendly, recyclable, and biodegradable since they are nontoxic, renewable, and biodegradable. Several interactions can also occur between these compounds and pollutants, such as electrostatic interactions, hydrogen bonds, π - π interactions, and stacking occurring between the functional groups. Water treatment applications can benefit

from natural polymers and GO in combination. This composite material has the ability to effectively purify water while addressing the problems caused by water pollution [4,5]. Ultimately, this can assist in supplying communities with clean and safe water.

Numerous dyes have been used to achieve significant economic gains. However, large amounts of dye wastewater are released into environmental water sources, thereby contaminating natural water sources [11]. The nitration and iodization of benzene, toluene, tea, and other raw materials to form intermediates, followed by the re-ammonization, coupling, and vulcanization of these intermediates, produces an industrial effluent. Due to the variety of dyes, pigments, and intermediates produced, the nature of the wastewater differs. Generally, they can be divided into acidic and alkaline wastewater. Many pollutants, such as sulfonation, nitrification, hydrogenation, reduction, oxidation, and acid (salt) precipitation, are generated during the dye production process. It is estimated that 90% of inorganic raw materials and 10–30% of organic raw materials in dye production are transferred to water, which is characterized by a high pollutant concentration, complex composition, high COD, high chroma, and strong alkalinity, and is one of the key environmental pollutants [18–20]. Therefore, effective degradation and treatment of dyes is an essential prerequisite for treating dye wastewater. Adsorbents have become the preferred material for industrial dye wastewater treatment applications because of their unique physical and chemical properties, powerful adsorption capacity, simplicity of preparation, controllable morphology and size, excellent strength, and easy regeneration. Many adsorbents with different controllable sizes, morphologies, and multifunctions have been designed, synthesized, and applied to the adsorption of various dyes. At present, activated carbon, ion exchange resins, and mesoporous molecular sieves are the most common adsorbents, and new nanomaterials are constantly being explored and developed. With the maturity of graphene theory and preparation technology, graphene with a large specific surface area and rich surface oxygen-containing functional groups obtained using new preparation methods has shown powerful adsorption capacity, which has great potential application value in treating organic wastewater and heavy metal ions [21].

Currently, the preparation technology of graphene is also constantly developing, especially the synthesis technology of graphene oxide as a precursor of graphene, which significantly strengthens the application ability of graphene in various fields [11–15]. Carbon atoms in nature have four valence electrons, and each carbon atom in graphene is an SP² hybrid. They can contribute to the unbonded π electrons. The π electrons and graphene were formed in a two-dimensional vertical plane, forming a conjugate orbit. The π electrons can move freely throughout the graphene plane, providing graphene with good electrical conductivity [18]. With the rapid development of nanotechnology, materials science, and molecular biology, biomimetic nanofluid systems with asymmetric ion transport properties and environmental adaptations have attracted great interest and have gained more functions. Potential applications in sensing, water purification, energy transmission, and other fields are limited.

This study presents the successful grafting of PANI polymer on the edge of graphene and tests its adsorption properties for MB and Pb²⁺. The results showed that at 298 K, the maximum adsorption capacity of GO-PANI was 1416 mg/g, 2.3 times that of PANI. The kinetic curves of PANI and GO-PANI adsorption of Pb (II) fit well with the quasi-second-order kinetic model, and the equilibrium adsorption curve conforms to the Langmuir adsorption isotherm. Additionally, the adsorption process was spontaneous, as AG was negative. This study also found that GO-PANI can effectively adsorb both Pb (II) and MB in mixed adsorption systems, with a maximum adsorption capacity for MB and Pb (II) of 544 mg/g and 1004 mg/g, respectively, after 90 min of adsorption. Ultimately, these findings allow for significant applications in sewage treatment. In addition to the presence of characteristic functional groups of both components, FT-IR analysis confirmed the success of graphene oxide–natural polymer composite synthesis. Furthermore, the interactions and bonds between GO and the natural polymer indicate that the two materials have a strong interface, which is likely to improve the adsorption capacity of the composites. Both GO

and the natural polymer exhibited diffraction peaks in the composite material, confirming the presence of crystalline phases. Consequently, the natural polymer did not degrade the crystal structure of the composites.

The FT-IR and XRD analyses of GO and the GO-PANI showed that it was successfully synthesized and had a crystalline structure. Based on these findings, it can be concluded that the composite material has desirable properties for adsorbing contaminants, mainly because of the enhanced adsorption capacity of GO and its potential synergistic effects with PANI. FT-IR spectra indicated that specific functional groups might act as adsorption sites for water contaminants. From the XRD results, we better understood the adsorption process and its stability as well as structural changes.

In this study, the FT-IR and XRD characterization results demonstrate that graphene oxide–natural polymer composites can be used in water treatment processes as adsorbent materials, highlighting their potential to tackle water pollution. The composite's adsorption performance, kinetics, and potential scalability should be further examined in real-world water treatment applications.

In this study, we successfully synthesized GO-PANI nanocomposites by attaching amino groups to GO surfaces and performing oxidative polymerization with aniline monomers. The addition rate of the oxidizing agent affected the morphology and performance of the resulting nanocomposites. Various characterization techniques such as XRD, TEM, and Raman spectroscopy were employed to analyze the properties of the GO-PANI nanocomposites. TEM was used to observe the morphologies of the GO, PANI, and GO-PANI. The results showed that GO-PANI had higher thermal stability and adsorption capacity for lead ions and organic dyes than PANI. The van der Waals equation curves were plotted to calculate the thermodynamic parameters ΔH , ΔS , and ΔG , which indicated that the adsorption of Pb (II) using PANI and GO-PANI was a spontaneous endothermic process. The co-adsorption experiment showed that GO-PANI had good adsorption capacity for MB and Pb (II) in a coexisting system. These findings provide insight into the development of graphene-based materials for environmental applications.

5. Conclusions

This work emphasizes the potential advantages of employing natural polymer composite adsorption materials for the purification of water, a problem that is becoming more crucial globally. Water quality may be significantly improved by applying GO–natural polymer composite adsorption materials. Heavy metals, organic contaminants, and microorganisms can be removed from water using the composite material in places with water contamination problems. Furthermore, the composite material is made from natural polymers and GO, which makes it a possible alternative to conventional water purification techniques since it is long-lasting and environmentally friendly. When it comes to reducing the environmental footprint and adopting ecofriendly practices, this could be particularly significant. By using GO–natural polymer composite adsorption materials in water treatment, a significant step can be achieved towards making water safe and clean.

Funding: This research received no external funding.

Data Availability Statement: The experimental data used to support the findings of this study are available from the corresponding author upon request.

Acknowledgments: The authors would like to show sincere thanks to the technicians who contributed to this research.

Conflicts of Interest: The author declare no conflict of interest.

References

1. Thakur, K.; Kandasubramanian, B. Graphene and graphene oxide-based composites for removal of organic pollutants: A review. *J. Chem. Eng. Data* **2019**, *64*, 833–867. [[CrossRef](#)]
2. Wang, Y.; Pan, C.; Chu, W.; Vipin, A.K.; Sun, L. Environmental remediation applications of carbon nanotubes and graphene oxide: Adsorption and catalysis. *Nanomaterials* **2019**, *9*, 439. [[CrossRef](#)] [[PubMed](#)]

3. Velusamy, S.; Roy, A.; Sundaram, S.; Kumar Mallick, T. A review on heavy metal ions and containing dyes removal through graphene oxide-based adsorption strategies for textile wastewater treatment. *Chem. Rec.* **2021**, *21*, 1570–1610. [[CrossRef](#)]
4. Marjani, A.; Nakhjiri, A.T.; Adimi, M.; Jirandehi, H.F.; Shirazian, S. Effect of graphene oxide on modifying polyethersulfone membrane performance and its application in wastewater treatment. *Sci. Rep.* **2020**, *10*, 2049. [[CrossRef](#)] [[PubMed](#)]
5. Huaping, Z.; Wu, T.; Sun, K.; Zhang, C. Towards High Accuracy Pedestrian Detection on Edge GPUs. *Sensors* **2022**, *22*, 5980.
6. Siddiqui, S.I.; Chaudhry, S.A. A review on graphene oxide and its composites preparation and their use for the removal of As³⁺ and As⁵⁺ from water under the effect of various parameters: Application of isotherm, kinetic and thermodynamics. *Process Saf. Environ. Prot.* **2018**, *119*, 138–163. [[CrossRef](#)]
7. Liu, Y.; Tu, W.; Chen, M.; Ma, L.; Yang, B.; Liang, Q.; Chen, Y. A mussel-induced method to fabricate reduced graphene oxide/halloysite nanotubes membranes for multifunctional applications in water purification and oil/water separation. *Chem. Eng. J.* **2018**, *336*, 263–277. [[CrossRef](#)]
8. Makhado, E.; Pandey, S.; Ramontja, J. Microwave assisted synthesis of xanthan gum-cl-poly (acrylic acid) based-reduced graphene oxide hydrogel composite for adsorption of methylene blue and methyl violet from aqueous solution. *Int. J. Biol. Macromol.* **2018**, *119*, 255–269. [[CrossRef](#)]
9. Chen, T.; Shi, P.; Zhang, J.; Li, Y.; Duan, T.; Dai, L.; Zhu, W. Natural polymer konjac glucomannan mediated assembly of graphene oxide as versatile sponges for water pollution control. *Carbohydr. Polym.* **2018**, *202*, 425–433. [[CrossRef](#)]
10. Chenab, K.K.; Sohrabi, B.; Jafari, A.; Ramakrishna, S. Water treatment: Functional nanomaterials and applications from adsorption to photodegradation. *Mater. Today Chem.* **2020**, *16*, 100262. [[CrossRef](#)]
11. Sherlala AI, A.; Raman AA, A.; Bello, M.M.; Buthiyappan, A. Adsorption of arsenic using chitosan magnetic graphene oxide nanocomposite. *J. Environ. Manag.* **2019**, *246*, 547–556. [[CrossRef](#)] [[PubMed](#)]
12. Wu, Z.; Huang, W.; Shan, X.; Li, Z. Preparation of a porous graphene oxide/alkali lignin aerogel composite and its adsorption properties for methylene blue. *Int. J. Biol. Macromol.* **2020**, *143*, 325–333. [[CrossRef](#)] [[PubMed](#)]
13. Lingamdinne, L.P.; Koduru, J.R.; Karri, R.R. A comprehensive review of applications of magnetic graphene oxide based nanocomposites for sustainable water purification. *J. Environ. Manag.* **2019**, *231*, 622–634. [[CrossRef](#)] [[PubMed](#)]
14. Wang, Z.; Gao, M.; Li, X.; Ning, J.; Zhou, Z.; Li, G. Efficient adsorption of methylene blue from aqueous solution by graphene oxide modified persimmon tannins. *Mater. Sci. Eng. C* **2020**, *108*, 110196. [[CrossRef](#)]
15. Wang, S.; Li, X.; Liu, Y.; Zhang, C.; Tan, X.; Zeng, G.; Jiang, L. Nitrogen-containing amino compounds functionalized graphene oxide: Synthesis, characterization and application for the removal of pollutants from wastewater: A review. *J. Hazard. Mater.* **2018**, *342*, 177–191. [[CrossRef](#)]
16. Sabzevari, M.; Cree, D.E.; Wilson, L.D. Graphene oxide–chitosan composite material for treatment of a model dye effluent. *ACS Omega* **2018**, *3*, 13045–13054. [[CrossRef](#)]
17. Ren, F.; Li, Z.; Tan, W.Z.; Liu, X.H.; Sun, Z.F.; Ren, P.G.; Yan, D.X. Facile preparation of 3D regenerated cellulose/graphene oxide composite aerogel with high-efficiency adsorption towards methylene blue. *J. Colloid Interface Sci.* **2018**, *532*, 58–67. [[CrossRef](#)]
18. Wang, S.; Ning, H.; Hu, N.; Huang, K.; Weng, S.; Wu, X.; Liu, J. Preparation and characterization of graphene oxide/silk fibroin hybrid aerogel for dye and heavy metal adsorption. *Compos. Part B Eng.* **2019**, *163*, 716–722. [[CrossRef](#)]
19. Xu, X.; Zou, J.; Zhao, X.R.; Jiang, X.Y.; Jiao, F.P.; Yu, J.G.; Teng, J. Facile assembly of three-dimensional cylindrical egg white embedded graphene oxide composite with good reusability for aqueous adsorption of rare earth elements. *Colloids Surf. A Physicochem. Eng. Asp.* **2019**, *570*, 127–140. [[CrossRef](#)]
20. Yuan, B.; Li, L.; Murugadoss, V.; Vupputuri, S.; Wang, J.; Alikhani, N.; Guo, Z. Nanocellulose-based composite materials for wastewater treatment and waste-oil remediation. *ES Food Agrofor.* **2020**, *1*, 41–52. [[CrossRef](#)]
21. Li, W.; Li, X.; Chang, W.; Wu, J.; Liu, P.; Wang, J.; Yu, Z.Z. Vertically aligned reduced graphene oxide/Ti₃C₂T_x MXene hybrid hydrogel for highly efficient solar steam generation. *Nano Res.* **2020**, *13*, 3048–3056. [[CrossRef](#)]
22. Wu, Z.; Deng, W.; Zhou, W.; Luo, J. Novel magnetic polysaccharide/graphene oxide@ Fe₃O₄ gel beads for adsorbing heavy metal ions. *Carbohydr. Polym.* **2019**, *216*, 119–128. [[CrossRef](#)] [[PubMed](#)]
23. Hossain, M.F.; Akther, N.; Zhou, Y. Recent advancements in graphene adsorbents for wastewater treatment: Current status and challenges. *Chin. Chem. Lett.* **2020**, *31*, 2525–2538. [[CrossRef](#)]
24. Maji, S.; Ghosh, A.; Gupta, K.; Ghosh, A.; Ghorai, U.; Santra, A.; Ghosh, U.C. Efficiency evaluation of arsenic (III) adsorption of novel graphene oxide@ iron-aluminium oxide composite for the contaminated water purification. *Sep. Purif. Technol.* **2018**, *197*, 388–400. [[CrossRef](#)]
25. Fu, W.; Wang, X.; Huang, Z. Remarkable reusability of magnetic Fe₃O₄-encapsulated C₃N₃S₃ polymer/reduced graphene oxide composite: A highly effective adsorbent for Pb and Hg ions. *Sci. Total Environ.* **2019**, *659*, 895–904. [[CrossRef](#)]

Disclaimer/Publisher’s Note: The statements, opinions and data contained in all publications are solely those of the individual author(s) and contributor(s) and not of MDPI and/or the editor(s). MDPI and/or the editor(s) disclaim responsibility for any injury to people or property resulting from any ideas, methods, instructions or products referred to in the content.